at the P3 stereotaxic level was similarly carried out in order to separate the lateral lemniscus complex from the superior olivary complex (*6*). In some cases, the cochlear nucleus was exposed by aspirating the overlying cerebellum and was then surgically isolated from the adjacent brainstem under visual control. The acoustic nerve was similarly isolated from the cochlear nucleus by carefully sectioning the nerve at the internal acoustic meatus. Each of these lesions was made with subsequent successful recordings in at least two animals. The animals were killed and were immediately perfused with 10 percent formalin. Frozen sections were cut at 80 μm and stained with thionine. Lesion reconstructions were made by projecting the relevant brain sections onto appropriate brain atlas diagrams (*6*).

In Fig. 1, the first trace indicates the typical sequence of far-field evoked response components elicited in the intact cat by binaural click stimuli. The average latency of each potential and its range were determined from recordings in seven cats, with the following values obtained: peak 1, 1.4 ± 0.2 msec; peak 2, 2.6 ± 0.3 msec; peak 3, 3.5 ± 0.4 msec; peak 4, 4.8 ± 0.5 msec; and peak 5, 6.7 ± 0.7 msec. Following decerebration, all potentials continued to be elicited at approximately the same amplitude and latency, which indicated that the primary loci of generation were caudal to the level of midbrain transection. Subsequent aspiration of the inferior colliculi or, in other experiments, isolation of the colliculi from the brainstem by bilateral undercutting eliminated potential 5 (Fig. 1). After stable recordings had been obtained from the acollicular preparation, the cochlear nucleus was surgically isolated from the adjacent brainstem. Following this procedure, potentials 3 and 4 disappeared, while potentials 1 and 2 continued to be elicited by the click stimuli at approximately control amplitude and latency. When the acoustic nerve was subsequently isolated from the cochlear nucleus, potential 2 disappeared while potential 1 continued to be elicited. This potential disappeared following a lethal dose of pentobarbital. These data indicated that potential 5 required the integrity of the inferior colliculus, while potentials 2 and 1 required the integrity of the cochlear nucleus and the acoustic nerve, respectively.

To assess the contribution of crossed projections, particularly to potentials 3 and 4, the split brainstem preparation was next studied. With binaural click stimulation, the typical sequence of evoked potential components was induced in the decerebrate cat with intact brainstem (Fig. 2). After sagittal midline section of the brainstem, there was little change in amplitude or latency of potentials 1 and 2. In contrast, potential 3 was largely abolished in the split brainstem preparation illustrated, even though a ventral fragment of the trapezoid body remained intact; in other preparations, with complete interruption of the trapezoid body, potential 3 was completely abolished. Potential 4 was reduced approximately 50 percent after the sagittal brainstem section and potential 5 largely disappeared. Hence, far-field potentials 1 and 2 were independent of fibers crossing the midline, whereas potentials 3 and 5 were largely dependent upon such crossed projections and potential 4 was approximately equally dependent upon crossed and uncrossed projections.

In order to analyze further the origins of potentials 3 and 4, sections were made between the lateral lemniscus and superior olivary complex before or after sagittal midline section. As noted above, far-field potentials 1, 2, and 4 remained following the sagittal brainstem section when click stimuli were delivered to the left or right ear. Subsequent transverse section of the left hemibrainstem, which destroyed the dorsal nucleus and interrupted the tract of the lateral lemniscus, produced no change in the potentials (Fig. 3, left clicks, A and B). In contrast, a section through the right hemibrainstem, which destroyed the ventral nucleus of the lateral lemnicus and the adjacent preolivary complex, resulted in the loss of potential 4 (Fig. 3, right clicks, A and B). When transverse sections were made bilaterally through the ventral nuclear region of the lateral lemniscus prior to the sagittal midline section, potential 4 was almost completely abolished, whereas potential 3 showed only a slight reduction in amplitude. Thus, potential 4 required the integrity of the ventral nucleus of the lateral lemniscus and the adjacent preolivary complex and was dependent to almost an equal extent upon the crossed and uncrossed projections to this area. Potential 3, in contrast, was dependent upon a more caudally situated structure which received primarily crossed inputs, which suggests the medial superior olivary nucleus as the primary generator of this potential.

These data indicate the primary origin of each of the far-field acoustic response components in the cat. Such identification may enhance the usefulness of this measure in both basic and clinical neurophysiological studies.

JENNIFER S. BUCHWALD
CHI-MING HUANG
Department of Physiology, Mental Retardation Center, and *Brain Research Institute, University of California Medical Center, Los Angeles 90024.*

References and Notes

1. D. L. Jewett, M. N. Romano, J. S. Williston, *Science* **167**, 1517 (1970); D. L. Jewett and J. S. Williston, *Brain* **94**, 681 (1971); H. Sohmer, M. Feinmesser, L. Banberger-Tell, A. Lev, S. David, *Dev. Med. Child Neurol.* **15**, 8 (1973); T. W. Picton, S. A. Hillyard, H. I. Krausz, R. Galambos, *Electroencephalogr. Clin. Neurophysiol.* **36**, 191 (1974).
2. D. L. Jewett, *Electroencephalogr. Clin. Neurophysiol.* **28**, 609 (1970).
3. A. Lev and H. Sohner, *Arch. Klin. Exp. Ohren. Nasen. Kehlkopfheilkd.* **201**, 79 (1972).
4. D. L. Jewett and M. N. Romano, *Brain Res.* **36**, 101 (1972).
5. K. Hecox and R. Galambos, *Arch. Otolaryngol.* **99**, 30 (1974).
6. A. L. Berman, *The Brain Stem of the Cat* (Univ. of Wisconsin Press, Madison, 1968).
7. Supported by PHS grants NS 05437, HD 04612, HD 05958, and NIH special resources grant RR-3.

25 November 1974; revised 11 February 1975

Tetrahedral Intermediate in a Specific α-Chymotrypsin Inhibitor Complex Detected by Laser Raman Spectroscopy

Abstract. *Laser Raman spectroscopy indicates that inhibition of α-chymotrypsin by 2-phenylethaneboronic acid occurs in two steps: (i) the formation of a loosely bound complex, in which the boron remains in a trigonal configuration; and (ii) reaction of the boron with a functional group in the catalytic site of the enzyme, resulting in a reversible, stable tetrahedral adduct.*

The design of a number of specific enzyme inhibitors has been based on the hypothesis that reactive intermediates, or transition states, of compounds whose reactions are being catalyzed bind considerably better to enzymes than do the compounds themselves (*1–3*). Among these compounds is 2-phenylethaneboronic acid, a powerful inhibitor of α-chymotrypsin, prepared by Koehler and Lienhard (*4*). These authors suggest that a tetrahedral adduct between the γ-oxygen of a serine residue in the catalytic site of the enzyme and the inhibitor is responsible for the strong binding, and they consider this intermediate analogous to the transition states of chymotrypsin-catalyzed reactions. However, a number of different boronic acid derivatives have been used as enzyme inhibitors (*5–6a*), and several mechanisms have been considered (*4, 6, 6a*) to account for their properties.

In view of the importance of boronic acids as specific enzyme inhibitors and their possible use in studies of mechanisms, we have investigated by means of laser Ra-

man spectroscopy the structure of a complex of crystalline α-chymotrypsin with 2-phenylethaneboronic acid.

The apparent dissociation constant of the crystalline complex formed with α-chymotrypsin and 2-phenylethaneboronic acid at *p*H 5.0 was determined by the indole displacement method (*7*). The value of 1.2 m*M* thus determined is comparable to a value of 1 m*M* obtained in solution studies at *p*H 5.0 (*4*).

The crystalline enzyme was specifically phosphorylated with diisopropyl phosphofluoridate under conditions known to lead to specific phosphorylation of the γ-oxygen of the serine residue in the active site of the enzyme (*8*). The laser Raman spectrum characteristic of the crystalline chymotrypsin–2-phenylethaneboronic acid complex (as described below) (Fig. 1c) at *p*H 7.0 was not seen when crystalline diisopropylphosphoryl α-chymotrypsin was used in the experiments.

The spectrum of 2-phenylethaneboronic acid in solution at *p*H 5.0 in the region between 547 cm^{-1} and 897 cm^{-1} is shown in Fig. 1a. A band is seen at 775 cm^{-1}. Also in Fig. 1a we see the solution spectrum of 2-phenylethaneboronic acid at high *p*H. There is a major band at 685 cm^{-1}. Spectra of solutions of methylboronic acid (*9*) under the same conditions are similar. The results were not affected by the presence of 60 percent (by volume) ammonium sulfate. Spectra of the trigonal boron compounds in solution and in a crystalline state appeared essentially the same in the spectral region examined.

The spectrum of chymotrypsin in the region between 650 cm^{-1} and 800 cm^{-1}, with a major band at 767 cm^{-1}, is seen in Fig. 1b. It is similar to the spectra of Lord and Yu (*10*) and Koenig (*11*). The spectra of a crystalline complex of α-chymotrypsin and 2-phenylethaneboronic acid at *p*H 5.5 and *p*H 7 are seen in Fig. 1c. At *p*H 7, a band at 684 cm^{-1} is observed, whereas this band is not observed at *p*H 5.5.

The specific and exclusive interaction of both diisopropyl phosphofluoridate and indole with the active site of chymotrypsin has been established by x-ray diffraction experiments (*8, 12*). We have used the two compounds to show that the laser Raman spectra discussed below refer to a specific chymotrypsin-inhibitor complex and to the interactions at the catalytic site.

A primary task in interpreting the laser Raman spectra was to identify the band at 685 cm^{-1} at high *p*H, and at 775 cm^{-1} at low *p*H, in the solution spectra of 2-phenylethaneboronic acid. Both bands appeared in the spectra of methylboronic acid with a similar structure and intensity. This confirms that the bands arise not from the methyl or phenylethyl groups but from the boronic acid. In addition, it is known that at *p*H 5.0 2-phenylethaneboronic acid is in the trigonal form, while at *p*H 11.0 it exists as a tetrahedral, negatively charged adduct with hydroxide ion (*13*). The exact nature of this vibration cannot be specified without a detailed spectroscopic and normal coordinate study of 2-phenylethaneboronic acid and its analogs. However, the frequency and polarization properties of the bands suggest that a boron-oxygen deformation may be responsible. In any event, the data indicate that the two bands do indeed arise from the boronic acid group and are sensitive to the *p*H-induced structural transition in 2-phenylethaneboronic acid (*13*).

The spectra obtained from the crystalline enzyme (Fig. 1b) were the best we have observed from a protein. The crystallization process appeared to have removed all fluorescent impurities. This reduced the background to a level which we believe is an inherent part of the Raman spectrum of the protein. At this level of purity, the amide I peak was three-and-a-half times the background. In essence, such sample purity allowed us to detect the relatively weak scattering of the 2-phenylethaneboronic acid in the active site of the enzyme.

With the spectral data shown in Fig. 1, a to c, as a basis, we tried to detect the vibration from the boronic acid group in a complex of α-chymotrypsin and 2-phenylethaneboronic acid at low and high *p*H.

At *p*H 5.5, where 2-phenylethaneboronic acid is known to bind less well by an order of magnitude than at *p*H 7.0, the

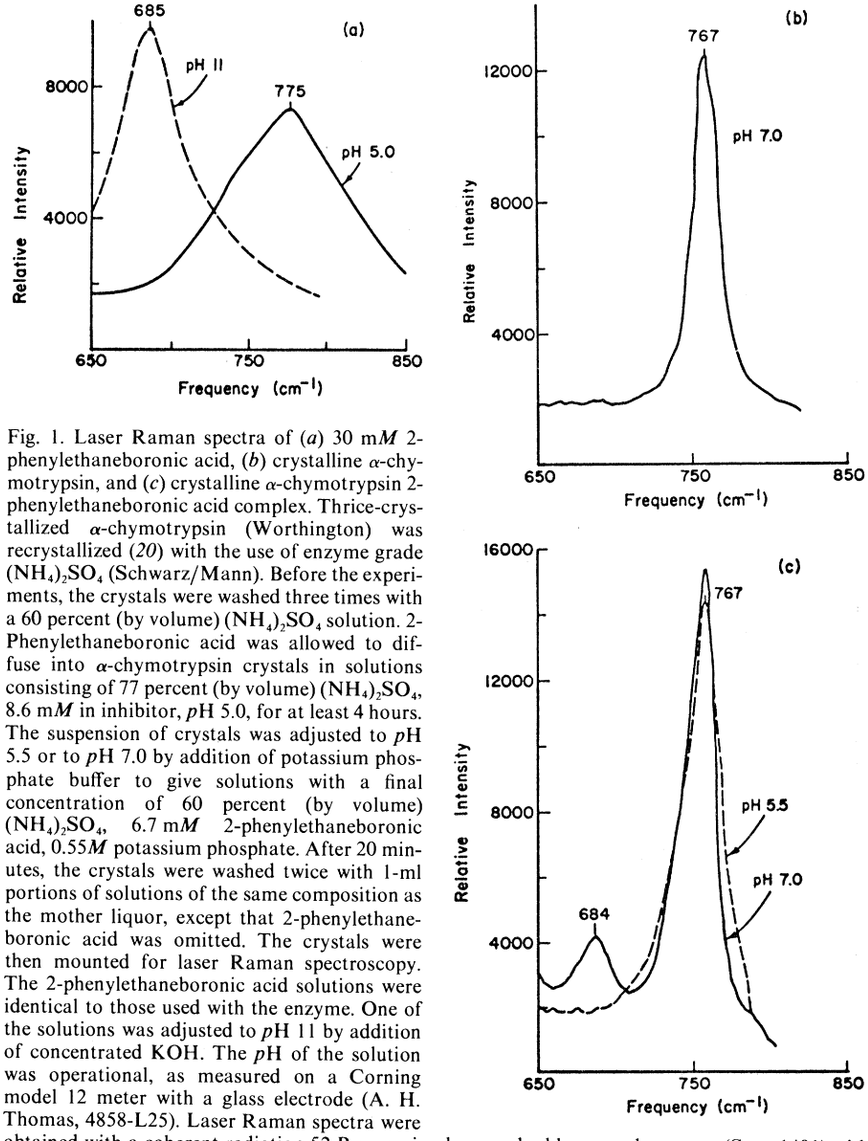

Fig. 1. Laser Raman spectra of (*a*) 30 m*M* 2-phenylethaneboronic acid, (*b*) crystalline α-chymotrypsin, and (*c*) crystalline α-chymotrypsin 2-phenylethaneboronic acid complex. Thrice-crystallized α-chymotrypsin (Worthington) was recrystallized (*20*) with the use of enzyme grade $(NH_4)_2SO_4$ (Schwarz/Mann). Before the experiments, the crystals were washed three times with a 60 percent (by volume) $(NH_4)_2SO_4$ solution. 2-Phenylethaneboronic acid was allowed to diffuse into α-chymotrypsin crystals in solutions consisting of 77 percent (by volume) $(NH_4)_2SO_4$, 8.6 m*M* in inhibitor, *p*H 5.0, for at least 4 hours. The suspension of crystals was adjusted to *p*H 5.5 or to *p*H 7.0 by addition of potassium phosphate buffer to give solutions with a final concentration of 60 percent (by volume) $(NH_4)_2SO_4$, 6.7 m*M* 2-phenylethaneboronic acid, 0.55*M* potassium phosphate. After 20 minutes, the crystals were washed twice with 1-ml portions of solutions of the same composition as the mother liquor, except that 2-phenylethaneboronic acid was omitted. The crystals were then mounted for laser Raman spectroscopy. The 2-phenylethaneboronic acid solutions were identical to those used with the enzyme. One of the solutions was adjusted to *p*H 11 by addition of concentrated KOH. The *p*H of the solution was operational, as measured on a Corning model 12 meter with a glass electrode (A. H. Thomas, 4858-L25). Laser Raman spectra were obtained with a coherent radiation 52 B argon ion laser, a double monochromator (Spex 1401) with a home-built stepping motor, and a multichannel analyzer (Nuclear Data model 1100). The photon counts recorded at each wavelength setting of the monochromator were plotted and averaged, with the aid of a PDP/11 minicomputer. With a counting time of 60 seconds, the background was a little more than 250 counts.

685 cm^{-1} band, characteristic of tetrahedral boron, is not seen in spectra of the crystalline enzyme-inhibitor complex (Fig. 1c). The indole displacement experiments, however, have shown that 2-phenylethaneboronic acid saturates the active site of the crystalline enzyme at *p*H 5.0. We conclude, therefore, that the intense α-chymotrypsin band at 767 cm^{-1} obscured the less intense band at 775 cm^{-1} because of trigonal boron in the chymotrypsin-inhibitor complex at *p*H 5.5 (Fig. 1c).

At *p*H 7.0, as is seen in Fig. 1c, the band at 684 cm^{-1} is present in the spectra of the crystalline enzyme-inhibitor complex. The position of the band at 684 cm^{-1} indicates that at this *p*H chymotrypsin binds 2-phenylethaneboronic acid in the tetrahedral configuration. X-ray studies indicate that in an analogous system, the crystalline complex of subtilisin BPN′ with 2-phenylethaneboronic acid, the inhibitor is bound to the active site of the enzyme in tetrahedral configuration (*14*).

These data and other results (*4–6, 15*) lead to the following interpretation of the inhibition mechanism. First an enzyme-inhibitor complex is formed in which the boron remains in trigonal form (*15*). The *p*H dependence of the inhibition, which has been reported to be similar to that observed in the catalytic reaction (*4, 6, 16*), occurs in a subsequent step which leads to a tetrahedral adduct between enzyme and inhibitor.

The tendency of boron to form weak complexes with a variety of functional groups is well known (*17–19*). Our data indicate that strong complex formation with a boronic acid derivative that can interact with the specific binding site of the enzyme and a functional group in the active site involves a tetrahedral adduct as suggested by Koehler and Lienhard (*4*).

GEORGE P. HESS
DAVID SEYBERT
Section of Biochemistry and Molecular Biology, Clark Hall, Cornell University, Ithaca, New York 14853
AARON LEWIS, JOHN SPOONHOWER
ROBERT COOKINGHAM
School of Applied and Engineering Physics, Clark Hall, Cornell University

References and Notes

1. L. Pauling, *Am. Sci.* **36**, 58 (1948).
2. R. Wolfenden, *Acc. Chem. Res.* **5**, 10 (1972).
3. G. E. Lienhard, *Science* **180**, 149 (1973).
4. K. A. Koehler and G. E. Lienhard, *Biochemistry* **10**, 2477 (1971).
5. V. K. Antonov, T. V. Ivaniva, I. V. Berezin, K. Martinek, *FEBS (Fed. Eur. Soc. Biochem.) Lett.* **7**, 23 (1970).
6. M. Philipp and M. L. Bender, *Proc. Natl. Acad. Sci. U.S.A.* **68**, 478 (1971).
7. J. D. Rawn and G. E. Lienhard, *Biochemistry* **13**, 3124 (1974).
8. L. A. Davis and G. P. Hess, *J. Mol. Biol.* **82**, 27 (1974).
9. P. B. Sigler, D. M. Blow, B. W. Matthews, R. Henderson, *ibid.* **35**, 143 (1968).
10. Gift of J. L. Fu.
11. R. C. Lord and N.-T. Yu, *J. Mol. Biol.* **51**, 203 (1970).
12. J. Koenig, *J. Polymer Sci.* **D60**, 59 (1972).
13. T. A. Steitz, R. Henderson, D. M. Blow, *J. Mol. Biol.* **46**, 337 (1968).
14. R. P. Bell, J. O. Edwards, R. B. Jones, in *The Chemistry of Boron and Its Compounds*, E. L. Muetterties, Ed. (Wiley, New York, 1967), chap. 4
15. We are grateful to Dr. J. Birktoft, Department of Chemistry, University of California, San Diego, for the communication of the unpublished results of D. Mathews, J. Birktoft, and J. Kraut.
16. K. A. Koehler and G. P. Hess, *Biochemistry* **13**, 5345 (1974).
17. For a recent review of this subject see G. P. Hess in *The Enzymes*, P. Boyer, Ed. (Academic Press, New York, 1971), vol. 3, p. 213.
18. R. Schaeffer, in *Progress in Boron Chemistry*, H. Steinberg and A. L. McCloskey, Eds. (Macmillan, New York, 1964), vol. 1, pp. 453–459.
19. D. W. Tanner and T. C. Bruice, *J. Am. Chem. Soc.* **89**, 6954 (1967).
20. K. A. Koehler, R. C. Jackson, G. E. Lienhard, *J. Org. Chem.* **37**, 2232 (1972).
21. P. B. Sigler, B. A. Jeffrey, B. W. Matthews, D. M. Blow, *J. Mol. Biol.* **15**, 175 (1966).

Supported by grant GM 04842 from the National Institutes of Health and grant GB 32483 from the National Science Foundation to G.P.H.; by a NSF graduate fellowship to D.S. (some of the experiments presented in this report were performed during a 6-week graduate student rotation program of the Section of Biochemistry); by a grant from the Research Corporation to A.L.; and by a fellowship from the Eastman Kodak Co. Inc., to J.S. 2-Phenylethaneboronic acid was generously supplied by Dr. G. E. Lienhard. We thank Miss Susan Coombs for growing α-chymotrypsin crystals.

19 August 1974; revised 25 February 1975

Anthopleurine: A Sea Anemone Alarm Pheromone

Abstract. *The sea anemone* Anthopleura elegantissima *responds with characteristic contraction to a pheromone released by wounded conspecifics. The alarm pheromone was isolated by ion-exchange chromatography and identified by chemical and spectroscopic methods as the quaternary ammonium ion (3-carboxy-2,3-dihydroxy-*N,N,N*-trimethyl)-1-propanaminium. Median effective concentration of the crystalline pheromone is 3.5 × 10^{-10} mole per liter of seawater.*

Evidence has been reported for the existence of pheromones in several marine invertebrates (*1*). With one exception the marine pheromones examined to date are large molecules not readily amenable to detailed chemical characterization (*2*). Unlike airborne pheromones that must be relatively small molecules to be volatile, waterborne pheromones need not be small to be soluble in water (*2*). The only marine pheromone whose structure is known is crustecdysone, a polar steroid that appears to be a sex pheromone in certain crabs (*3*).

We now report the discovery, isolation, and chemical structure of an alarm pheromone in the sea anemone *Anthopleura elegantissima* (Cnidaria, Anthozoa).

The aggregating form of *A. elegantissima* was collected from exposed intertidal rocks in Monterey, California. Animals from the single clone (*4*) used for bioassays were transferred in groups of six animals to 24 glass bowls (250 ml) and maintained in the laboratory with running seawater for 2 months before being used for experiments. An average illumination of 2300 lux

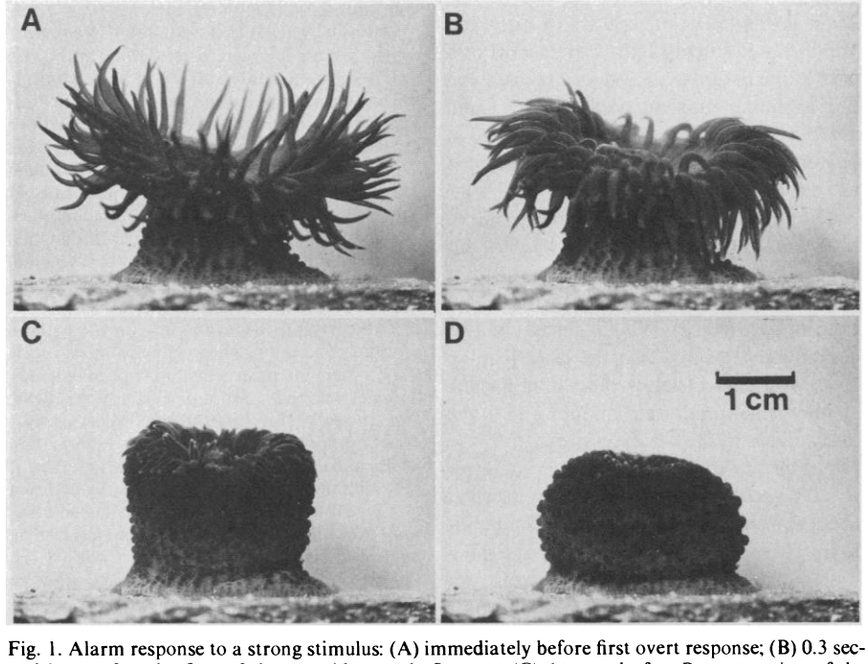

Fig. 1. Alarm response to a strong stimulus: (A) immediately before first overt response; (B) 0.3 second later, after the first of three rapid tentacle flexures; (C) 1 second after B, contraction of the mesenterial retractors; (D) 1.5 seconds after C, constriction of the marginal sphincter.